Appl. Phys. B 68, 807–812 (1999) / DOI 10.1007/s003409901485

Applied Physics B
Lasers
and Optics

Fermi-level engineering of $BaTiO_3$ by alkali codoping: increasing the near-infrared absorption by rhodium

R. Scharfschwerdt[1], **O.F. Schirmer**[1], **H. Hesse**[1], **D. Rytz**[2]

[1] Fachbereich Physik, Universität Osnabrück, D-49069 Osnabrück, Germany
(Fax: +49-541/969-2670, E-mail: schirmer@physik.uni-osnabrueck.de)
[2] Forschungsinstitut für mineralische und metallische Werkstoffe, Edelsteine/Edelmetalle GmbH, Struthstr. 2, Wackenmühle,
D-55743 Idar-Oberstein, Germany

Received: 18 November 1998/Revised version: 23 December 1998/Published online: 7 April 1999

Abstract. Using electron paramagnetic resonance, optical absorption, and fast spectroscopy of light-induced absorption changes, it is shown that codoping $BaTiO_3$:Rh with Na_{Ba} acceptors raises the charge state of Rh^{3+} to Rh^{4+}. Subsequent oxidation under high oxygen pressures can lower the Fermi level to $Rh^{4+/5+}$, leading to increased infrared absorption. The light-induced charge transfer in such specimens is characterised by “one center” behaviour.

PACS: 71.55.-i; 77.84.Dy; 78.40.Ha

Since 1993 it has been known [1, 2] that doping $BaTiO_3$ (BT) with Rh increases the photorefractive efficiency of this material in the near infrared. This discovery led to the realisation of various novel photorefractive schemes [3–6]. In several publications [7–12] the photorefractive properties of BT, as related to Rh doping, have been studied on a phenomenological basis. The defect chemical foundation of these properties was established by investigating the EPR of Rh^{4+} in BT [13] and by a combined investigation of the light-induced changes of EPR and optical absorption [14, 15]. In this way, the optical bands responsible for the photorefractive sensitivity have been correlated to the various occurring charge states of Rh. It turned out that the following three valencies are involved: Rh^{5+}, causing a charge transfer absorption peaked at 1.6 eV, Rh^{4+} with a band at 1.9 eV, and Rh^{3+}, whose absorption could not yet be identified. It is probably covered by the band-to-band transitions in BT. Light-induced charge transfers among these charge states are described by the “three-valence model” [16]. The infrared sensitivity of the material is mainly determined by the low-energy wings of the Rh^{5+} band. In order to increase the infrared response of the material it is thus necessary to raise the Rh^{5+} content in relation to the other charge states.

It will be shown in this paper that this can be achieved by incorporating alkali acceptor ions, for example Na^{+}_{Ba}, into the crystals. Especially if such specimens are strongly oxidised, the Fermi level can be lowered to such an extent, that only the charge states Rh^{4+} and Rh^{5+} occur and a turnover to “one-center” behavior [16] takes place; i.e. no light-induced absorptions are observed at room temperature.

The present paper will describe the influence of Na doping on the valencies of Rh, on the related changes of the Fermi level, E_F, and on the light-induced charge transfer paths, as depending on the oxidising treatment of the material and on crystal temperature. As an introductory example also the charge changes of Fe caused by Na doping will be dealt with. The emphasis will be on the qualitative evaluation of the experimental results. The paper will be organised in the following way: After an introduction to the defect chemical background the methods of the experimental investigations are described. Some specific results will then be presented and a summary of the findings be given.

1 Defect chemical background

Because optical absorptions in crystals with strong electron–phonon coupling, such as BT, are governed by the Franck–Condon principle (Fig. 1, left side), it is not astonishing that the thermal levels of Rh in BT are different from the peak energies of the optical bands. The level $Rh^{4+/5+}$, i.e. the position of the Fermi level at which both charge states can coexist in the crystal, has been inferred to lie at about 0.7 eV [14] above the valence band edge, whereas $Rh^{3+/4+}$ is assumed to be near 1.0 eV [7]. Both are different from the optical peak positions mentioned above. For most purposes in this paper the level scheme will be used in the symbolised form shown in Fig. 1 (right side), comprising all transitions, optical as well as thermal, to and from a defect level to the neighboring valence band.

The thermal levels of the alkali acceptors, $(Na^{+}_{Ba})'$ [17] and $(K^{+}_{Ba})'$, lie very close, about 50 meV, above the valence band edge [18]; the corresponding optical absorption is peaked at 1.3 eV [18]. Holes captured at such levels are thermally ionised at low temperatures near 35 K [18]. Such

---

Dedicated to Prof. Dr. Eckard Krätzig on the occasion of his 60th birthday.

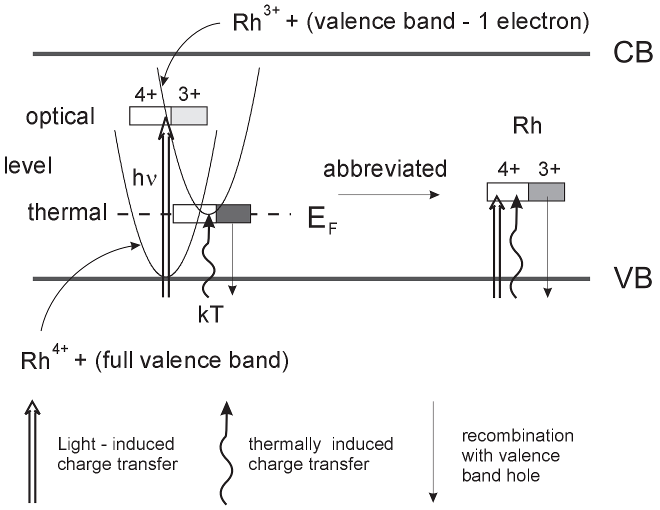

Fig. 1. *Left side*: Visualisation of the difference between optical and thermal levels of a defect. Two coordinates are superimposed along the abscissa: the spatial coordinate, depending on which the band scheme is plotted, and a configuration coordinate, depending on which the elastic energies corresponding to the two indicated charge configurations of the defect are shown. For most purposes this detailed structure is symbolised (*right side*) by one level, interacting with the valence band by light- and thermally induced electron excitation and recombination. The arrows indicate the directions of electron flow

acceptors should thus be ideally suited for lowering E_{F}. This means, by codoping BT:Rh with Na one can expect to stabilise the higher charge states of Rh. Such a Fermi-level engineering is commonly used in the classical semiconductors, employing suitable shallow donors or acceptors. For most oxide materials the formation of donors is easily achieved by chemical reduction. It is expected that oxygen vacancies, $V_{\mathrm{o}}^{\bullet\bullet}$, are formed in this way, introducing levels that are rather shallow with respect to the conduction band edge. Electrons at such levels will thus be thermally ionised at room temperature, lowering the valencies of defects lower in the gap. Using the shallow alkali acceptors, on the other hand, the charge states of deeper defects will be raised. The combination of both types of defects then should allow one to sweep the Fermi level over almost the entire gap of BT.

In crystals grown in a normal atmosphere, the acceptors – negatively charged with respect to the lattice – are assumed to be compensated by $V_{\mathrm{o}}^{\bullet\bullet}$ [19]. The ability of the acceptors to lower E_{F} is mostly latent at this stage. They become active under an oxidising treatment; then the Vo are filled by oxygen, and the positive charges of $V_{\mathrm{o}}^{\bullet\bullet}$ are replaced by holes which are captured at deep defects, raising their valencies. It will be shown in this paper, however, that a Na doping can lower E_{F} already to a certain degree before oxidation.

2 Experimental details

The most detailed information on the geometrical, chemical, electronic, and energetic structure of a paramagnetic defect can in favorable cases be obtained by electron paramagnetic resonance (EPR). We perform such measurements at temperatures between 4.2 K and 295 K with a Bruker 200 D SRC spectrometer, operating near 9 GHz. The results on BT:Fe, presented below, depend on measurements of EPR directly.

Table 1. The investigated crystals and their Rh and Na content (all values in mol ppm in the melt)

Crystal	Rh content	Na content
GG8	1000	10 000
GG9	3000	10 000
X16	1000	1000
X17	1000	1000
X14	1000	500
G50	1000	0

The other method used, the fast measurement of light-induced absorption changes, employs a homebuilt setup [20], which allows us to monitor the absorption status of a crystal in the range of 300 nm to 1100 nm within 20 ms. For a detailed description of the spectrometer and its use the reader is referred to [20]. This setup is easily adapted to the EPR spectrometer, and the light-induced EPR changes can be monitored almost simultaneously with the corresponding absorption changes. In this way the optical absorption bands can be correlated to the defects causing them. Investigations with this method have been published for $BaTiO_3$:Fe [21, 22] and for $BaTiO_3$:Rh [14, 15, 20]. On this basis we can now recognize most of the Rh charge states by their optical absorption bands. Therefore we can rely in this paper almost exclusively on optical investigations using the above fast spectrometer. Some plain optical absorption measurements have also been performed.

The investigated crystals had the Rh and Na concentrations shown in Table 1. They were investigated in their ‘as-grown’ state and after oxidation in pure O_2, with pressures of 10^5 Pa and 20×10^5 Pa, typically at 900 °C for 2 h. After such annealings the crystals were fast cooled without changing the oxygen pressure.

3 Introductory example: Fermi-level engineering by Na doping of $BaTiO_3$:Fe

Figure 2 shows the change of the charge states of Fe, observed by EPR, as caused by a Na doping and subsequent oxidation. Since the charge changes of this system can entirely be investigated by EPR, we use it for later comparison with BT:Rh, were the argumentation has to be based on optical bands. EPR can monitor the charge states Fe^{3+} and Fe^{5+}; the valencies Fe^{4+} and Fe^{2+} are EPR-silent. In part 2a, the EPR of Fe^{3+} (ground state $^6S_{5/2}$) in the untreated crystal, doped with iron, is seen. The spectrum is typical for this charge state, showing the fine-structure splittings $|1/2\rangle \leftrightarrow |3/2\rangle$, $|3/2\rangle \leftrightarrow |5/2\rangle$, etc., broadened by internal strains, in addition to the sharp $|+1/2\rangle \leftrightarrow |-1/2\rangle$ transition of Fe^{3+} [13]. No additional spectrum is observed with a crystal jointly doped with Fe and Na. Evidently, the Na acceptor still is latent and thus E_{F} remains pinned by the $Fe^{3+/4+}$ level. The negative charge of $(Na^+)'$ apparently is compensated by the necessary concentration of $V_{\mathrm{o}}^{\bullet\bullet}$ centers. After oxidation (in 20×10^5 Pa pure oxygen) the V_{o} are filled and the compensation proceeds by holes, partly captured at Fe^{3+}, forming Fe^{4+}, and partly at Fe^{4+}, leading to Fe^{5+}. The corresponding shift of E_{F} is demonstrated by the vanishing of the EPR of Fe^{3+} and the presence of Fe^{5+}, indicating that E_{F} is pinned at $Fe^{4+/5+}$.

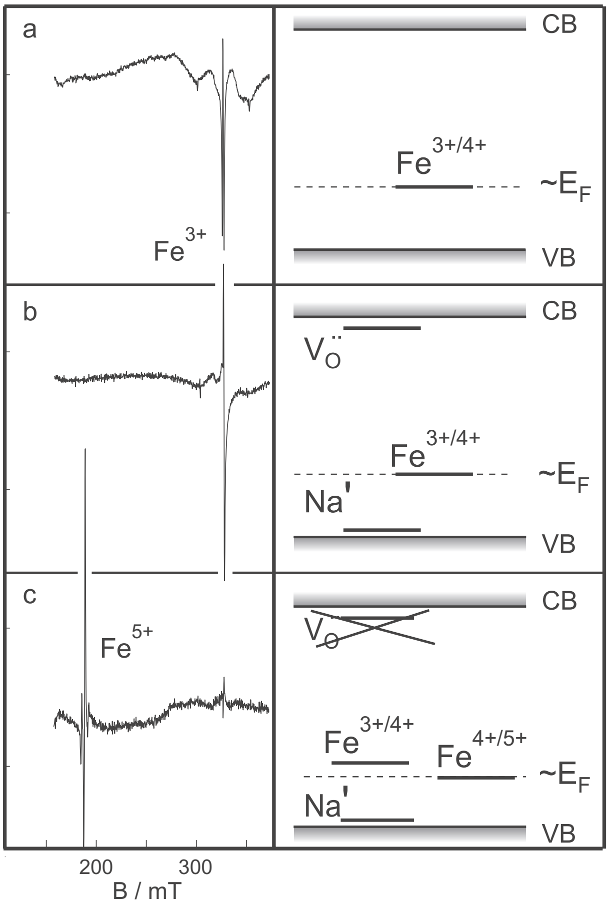

Fig. 2a–c. The valencies of Fe in $BaTiO_3$, depending on Na doping and oxidation, as studied by EPR. **a** Without Na doping: Only Fe^{3+} is observed; the Fermi level is pinned by $Fe^{3+/4+}$. **b** With Na doping: The Na' acceptor is compensated by $V_\text{o}^{\bullet\bullet}$ and thus does not raise the valencies of Fe. **c** By oxidation (20×10^5 Pa, 900 °C) the $V_\text{o}^{\bullet\bullet}$ are filled and compensation is achieved by formation of Fe^{5+}, as observed by EPR

4 Investigation of $BaTiO_3$:Rh, Na

4.1 *Optical absorption*

Figure 3 shows the influence of a Rh and Na doping as well as oxidation under 20×10^5 Pa oxygen on the optical absorption of the indicated $BaTiO_3$:Rh, Na crystals. Annealing under an oxygen pressure of 10^5 Pa usually does not lead to decisive changes as compared to the ‘as-grown’ crystals. Therefore we do not deal further with results obtained with such slightly oxidised specimens. From Fig. 3 it is seen that the incorporation of Na in addition to Rh leads to an increase of the Rh^{4+} absorption at 1.9 eV already before oxidation (crystal X17). This means that previously Rh^{3+} must have been present, balanced by an unknown donor, probably an oxygen vacancy. The newly created Rh^{4+}, having the same valency as the replaced Ti^{4+}, does not need to be compensated. The incorporated Na', however, can be assumed to be balanced by $V_\text{o}^{\bullet\bullet}$, as also found for the case of BT:Fe. After strong oxidation, as studied with crystal X16 (composition nominally the same as that of X17), all compensation of Na' is then effected by the increased concentration of Rh^{5+}. The presence of the latter is inferred from difference spectra, Fig. 3, lower part.

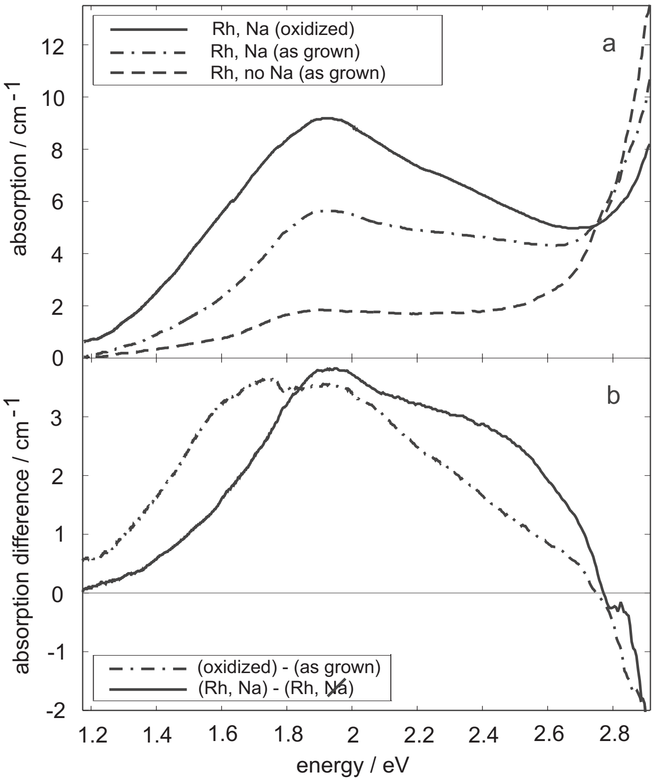

Fig. 3a,b. Optical absorption of BT:Rh, depending on Na doping and oxidation. **a** Absorption spectra of BT:Rh, of BT:(1000 ppm Rh), (1000 ppm Na), and of BT:Rh, Na after oxidation with 20×10^5 Pa O_2. Initially Rh^{4+} (band at 1.9 eV) and Rh^{3+} (low-energy wing of fundamental absorption) is present; the Fermi level is pinned by $Rh^{3+/4+}$. By Na doping alone the absorption of Rh^{4+} increases, that of Rh^{3+} decreases. After oxidation also a band of lower energy, attributable to Rh^{5+} is observed

It is also seen from this figure that a Na doping decreases the absorption near 2.9 eV; the transparency in this range is further increased by additional oxidation. These features are in accord with the assumption that the Rh^{3+} absorption in $BaTiO_3$ is covered by the band-to-band transitions. The wings of the Rh^{3+} band, extending slightly below the fundamental absorption edge, decrease as expected under the indicated treatments. The difference spectra again show that the Rh^{4+} band near 1.9 eV increases after Na doping, consistent with the decrease of the Rh^{3+} absorption. In addition, a wide absorption near 2.5 eV rises, which can possibly be attributed to the formation of Fe^{5+} [14]. Under oxidation the Rh^{4+} band rises further and also a band near 1.6 eV, caused by Rh^{5+}, appears.

4.2 *Light-induced optical absorption changes*

The light-induced absorption changes are also affected by the Na doping and oxidation treatments. The analysis of these observations gives further insight into the accompanying changes of the Rh charge states. We shall present two representative examples.

Figure 4 shows the light-induced absorption changes of the crystal X16 in the as-grown state, observed at 15 K. In the middle part of the figure the absorption changes are plotted resulting from illumination with various energies of high-intensity pump light. Seventeen different energies were used

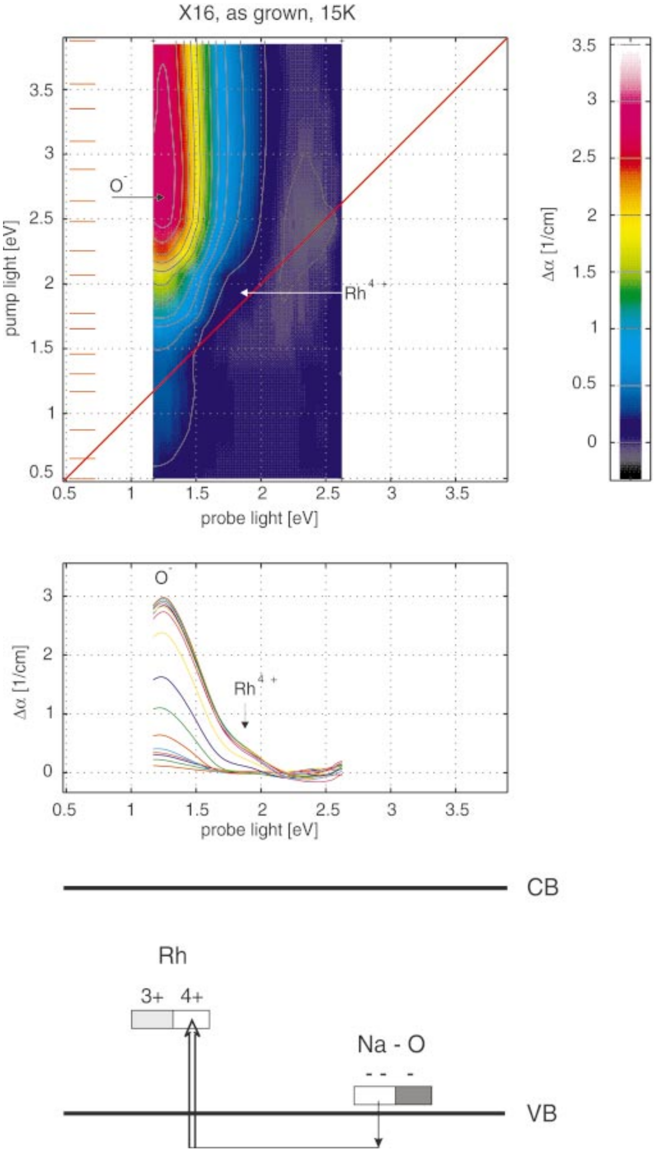

Fig. 4. Absorption changes of BT:Rh, Na at 15 K, depending on pump light energies, see text. Strong absorption at 1.3 eV, caused by Na – O^-, is observed; the concentration of Rh^{4+} decreases as indicated by the downward kink, superimposed on the O^- absorption. The corresponding charge transfer path is indicated in the lower panel

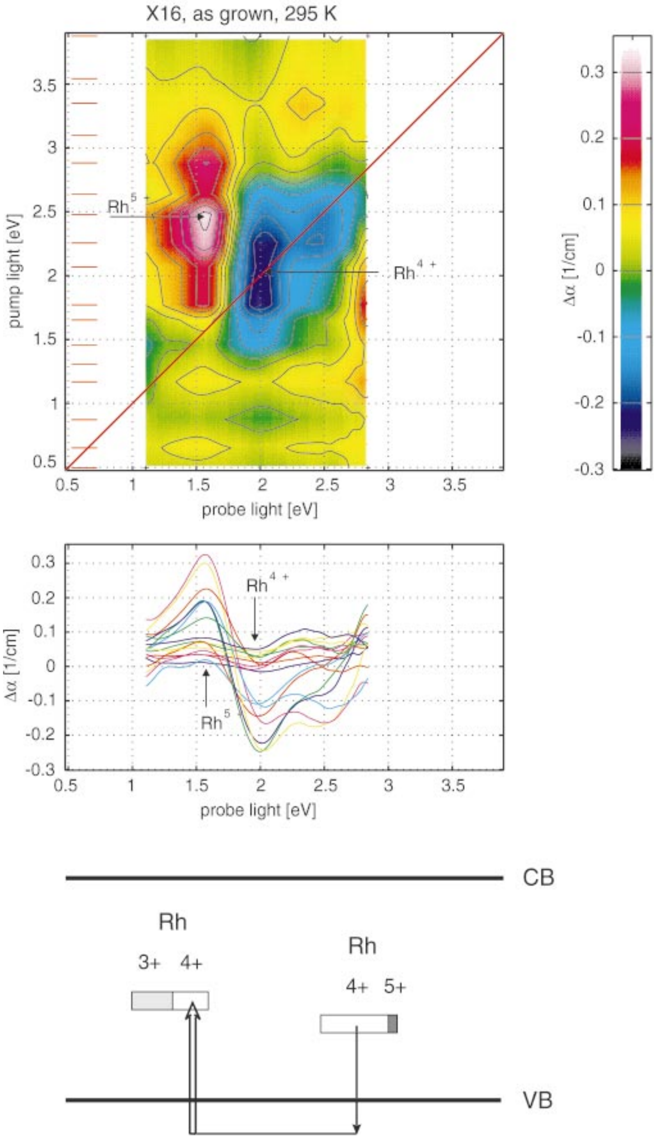

Fig. 5. Light-induced absorption changes of the same crystal as in Fig. 4, now at room temperature. The light-induced processes are started by the excitation of a valence band electron to Rh^{4+}, decreasing the corresponding absorption; the hole created in this way is trapped by another Rh^{4+}, and Rh^{5+} forms

and subsequently applied to the specimen, starting with the lowest energy, 0.5 eV. Immediately after each pump illumination, lasting 60 s, the induced absorption changes were monitored within 20 ms using wide-band weak probe light.

A clearer presentation of the same information as in the middle part is given by a pseudo-3D plot in the upper part. The absorption changes are given by a color code, defined at the right of each figure. The seventeen pump light energies used are given as short horizontal lines along the ordinate whereas the probe light energies again extend along the abscissa. One absorption spectrum, as in the middle panel of the figure, corresponds to each of the used pump light energies. The continuous 3D plot in the upper part is obtained by numerical interpolation between the separate curves. Starting from the lowest pump energies, significant rises in absorption at $E_{\text{probe}} = 1.3$ eV start at $E_{\text{pump}} = 1.5$ eV and increase further up to $E_{\text{pump}} = 2.9$ eV. This band at $E_{\text{probe}} = 1.3$ eV has been assigned previously to $O^- – Na^+$ [18]. Light-induced absorption decreases lying on the diagonal, indicated in the figure, correspond to primary photoprocesses [20], i.e. to those driving a light-induced reaction. The deformation of the “mountain” of the 1.3 eV absorption near the diagonal at 1.9 eV is attributed to a superimposed transparency caused by a decrease of the Rh^{4+} absorption. The same feature is also indicated by the downward kink near 1.9 eV in the middle panel. Figure 4 thus has to be interpreted as in the lowest panel: Electrons are excited by light from the valence band to Rh^{4+} and the holes created in this way are captured at O^- next to Na^+. These holes are stable at this site at 15 K, leading to the high absorption changes observed. The Fermi level apparently is pinned by $Rh^{3+/4+}$.

At room temperature the holes, created by pump light, are not stable at the $Na^+ – O^-$ acceptor and they thus are captured at a deeper level. For X16, as-grown, Fig. 5, it is observed that pump light again decreases the Rh^{4+} concentration; but the holes are now trapped by another Rh^{4+} ion, leading to Rh^{5+}, as evidenced by the corresponding absorption increase at 1.6 eV. During the described process also Rh^{3+} is created, covered by the fundamental absorption. The described light-induced absorption changes are typical for a three-valence model.

If specimen X16 is now strongly oxidised, hardly any absorption changes are observed, Fig. 6. This is an indication that a one-center situation [16] has been achieved, as indicated in the lower panel of that figure. By strong oxidation the negative charges of the Na' acceptors are compensated by Rh^{5+}; the Fermi level has correspondingly shifted downward to the $Rh^{4+/5+}$ level. Electrons are excited from the valence band to the Rh^{5+} and the created holes are trapped by Rh^{4+} at another site and there is no net optical absorption change. Such a one-center behavior has been observed for all crystals with a [Rh]/[Na] ratio < 2 after annealing in oxygen with 20×10^5 Pa pressure.

Summarising, we have found:

- unless the crystals are oxidised under high oxygen pressure, the light-induced charge transfer processes in BT:Rh take place according to the three-valence model, involving Rh^{3+}, Rh^{4+}, and Rh^{5+}
- for crystals pulled from melts containing a [Rh]/[Na] ratio < 2 one-center behavior is observed after strong oxidation. In this case E_F is lowered to $Rh^{4+/5+}$.
- in some crystals a weak optical absorption of $O^- – Na^+$ has been observed without prior illumination, if the specimens had been strongly oxidised. Since simultaneously the optical band of Rh^{4+} was monitored, this does not mean that the material had an essentially unactivated p-conductivity, characterised by E_F lying in the valence band or near the Na acceptor level. The optical absorption of O^- – Na rather results from the thermal equilibrium hole distribution between the $Rh^{4+/5+}$ and the Na acceptor levels at room temperature
- in crystals grown from melts having a low ratio of Rh/Na, such as GG8, GG9, and X17, the concentration of Rh^{4+} is increased already by Na doping without subsequent oxidation. This means that not all of the Na' acceptors are compensated by $V_o^{\bullet\bullet}$ but by the higher valencies of Rh.

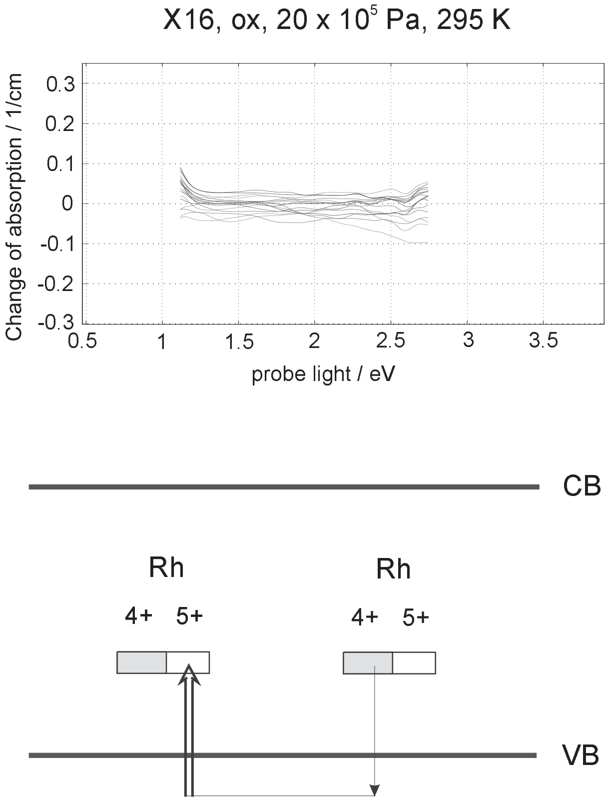

Fig. 6. With the same crystal as in Fig. 5 essentially no light-induced absorption is observed after oxidation under an O_2 atmosphere of 20×10^5 Pa. The Fermi level is pinned by $Rh^{4+/5+}$ and a "one-center" situation is present, as indicated by *the lower panel*

5 Influence of background impurities

It should be noted that the valencies and charge transfer paths in the investigated crystals can be decisively influenced by the presence of unintended background impurities. In specimen X16, for instance, EPR has identified the presence of Fe, Cr, and Pt in addition to Rh and Na. Furthermore there is evidence that there are additional defects which are EPR-silent. The light-induced charge transfer processes are most strongly influenced by the formation of Fe^{5+} and by an unidentified defect leading to optical absorption changes at 2.2 eV. The effect of such impurities can cause decisive deviations from the standard behavior for light-induced absorption changes as described above. The optimisation of photorefractive BT:Rh thus has to consider also how these unwanted background impurities can be avoided.

6 Conclusion

We have shown that codoping BT with Na as well as Rh leads to an increase of the Rh valencies, especially if such crystals are oxidised under high oxygen pressures. In most of the cases the latter treatment causes a shift of E_F from the $Rh^{3+/4+}$ level to $Rh^{4+/5+}$. It has been shown recently [23] that such an oxidation can decisively shorten the photorefractive response time of the material. It was furthermore found that background impurities have a strong influence on the light-induced charge transfer phenomena in such crystals.

Acknowledgements. We thank W. Koslowski, M. Maiwald, A. Mazur, and C. Veber for help during the preparation of the manuscript. To G.I. Malovichko we are grateful for helpful comments. N. Huot kindly communicated experimental information. The work described here was supported by DFG in the frame of SFB 225 and TFB 13.

References

1. B.A. Wechsler, M.B. Klein, C.C. Nelson, R.N. Schwartz: Opt. Lett. **19**, 36 (1994)
2. G.W. Ross, P. Hribek, R.W. Eason, M.H. Garrett, D. Rytz: Opt. Commun. **101**, 60 (1993), In this paper optical absorption was identified which later turned out to be caused by Rh^{4+}
3. S. MacCormack, G.D. Bacher, J. Feinberg, S. O'Brien, R.J. Lang, M.B. Klein, B.A. Wechsler: Opt. Lett. **22**, 227 (1997)
4. A. Brignon, J.-P. Huignard, M.H. Garrett, I. Mnushkina: Opt. Lett. **22**, 215 (1997)
5. N. Huot, J.M.C. Jonathan, D. Rytz, G. Roosen: Opt. Commun. **140**, 296 (1997)
6. N. Huot, J.M.C. Jonathan, G. Roosen, D. Rytz: Opt. Lett. **22**, 976 (1997)
7. U. van Stevendaal, K. Buse, S. Kämper, H. Hesse, E. Krätzig: Appl. Phys. B **63**, 315 (1996)
8. M. Kaczmarek, P. Hribek, R.W. Eason: Opt. Commun. **136**, 277 (1997)
9. L. Corner, R. Ramos-Garcia, A. Petris, M.J. Damzen: Opt. Commun. **143**, 165 (1997)
10. H. Song, S.X. Dou, M. Chi, H. Gao, Y. Zhu, P. Ye: J. Opt. Soc. Am. B **15**, 1329 (1998)
11. N. Huot, J.M.C. Jonathan, G. Pauliat, D. Rytz, G. Roosen: Opt. Commun. **135**, 133 (1997)
12. N. Huot, J.M.C. Jonathan, G. Roosen: Appl. Phys. B **65**, 489 (1997)
13. E. Possenriede, P. Jacobs, O.F. Schirmer: J. Phys. C **4**, 73 (1992)
14. H. Kröse, R. Scharfschwerdt, O.F. Schirmer, H. Hesse: Appl. Phys. B **61**, 1 (1995)
15. H. Kröse, E. Possenriede, R. Scharfschwerdt, T. Varnhorst, O.F. Schirmer, H. Hesse, C. Kuper: Opt. Mater. **4**, 153 (1995)
16. K. Buse: Appl. Phys. B **64**, 273 (1997)
17. Here and in the following sometimes the Kröger–Vink notation is used in order to indicate the defect charges relative to the unperturbed lattice
18. T. Varnhorst, O.F. Schirmer, H. Kröse, R. Scharfschwerdt: Phys. Rev. B **53**, 116 (1996)
19. D.M. Smyth: Prog. Solid State Chem. **15**, 145 (1984)
20. H. Kröse, R. Scharfschwerdt, A. Mazur, O.F. Schirmer: Appl. Phys. B **67**, 79 (1998)
21. A. Mazur, U. van Stevendaal, K. Buse, M. Weber, O.F. Schirmer, H. Hesse, E. Krätzig: Appl. Phys. B **65**, 481 (1997)
22. A. Mazur, O.F. Schirmer, S. Mendricks: Appl. Phys. Lett. **70**, 2395 (1997)
23. N. Huot, G. Pauliat, J.M.C. Jonathan, G. Roosen, R. Scharfschwerdt, O.F. Schirmer: CLEO/EUROPE-EQEC '98, paper CFE2